

Received:
22 October 2014

Revised:
2 February 2015

Accepted:
26 March 2015

doi: 10.1259/bjr.20140660

Cite this article as:

Jones A, Ansell C, Jerrom C, Honey ID. Optimization of image quality and patient dose in radiographs of paediatric extremities using direct digital radiography. *Br J Radiol* 2015;88:20140660.

FULL PAPER

Optimization of image quality and patient dose in radiographs of paediatric extremities using direct digital radiography

^{1,2}A JONES, BSc, MSc, ³C ANSELL, BSc, MSc, ¹C JERROM, MPhys, MSc and ¹I D HONEY, MPhys, MSc

¹Medical Physics Department, Guy's and St Thomas' NHS Foundation Trust, London, UK

²Medical Physics Department, Western Sydney Local Health District, Sydney, NSW, Australia

³Radiology Department, Evelina London Children's Hospital, Guy's and St Thomas' NHS Foundation Trust, London, UK

Address correspondence to: Mr Adam Jones

E-mail: adam.jones@gstt.nhs.uk

Objective: The purpose of this study was to evaluate the effect of beam quality on the image quality (IQ) of ankle radiographs of paediatric patients in the age range of 0–1 year whilst maintaining constant effective dose (ED).

Methods: Lateral ankle radiographs of an infant foot phantom were taken at a range of tube potentials (40.0–64.5 kV_p) with and without 0.1-mm copper (Cu) filtration using a Trixell Pixium 4600 detector (Trixell, Morains, France). ED to the patient was computed for the default exposure parameters using PCXMC v. 2.0 and was fixed for other beam qualities by modulating the tube current-time product. The contrast-to-noise ratio (CNR) was measured between the tibia and adjacent soft tissue. The IQ of the phantom images was assessed by three radiologists and a reporting radiographer. Four IQ criteria

were defined each with a scale of 1–3, giving a maximum score of 12. Finally, a service audit of clinical images at the default and optimum beam qualities was undertaken.

Results: The measured CNR for the 40 kV_p/no Cu image was 12.0 compared with 7.6 for the default mode (55 0.1 mm Cu). An improvement in the clinical IQ scores was also apparent at this lower beam quality.

Conclusion: Lowering tube potential and removing filtration improved the clinical IQ of paediatric ankle radiographs in this age range.

Advances in knowledge: There are currently no UK guidelines on exposure protocols for paediatric imaging using direct digital radiography. A lower beam quality will produce better IQ with no additional dose penalty for infant extremity imaging.

Long bones (arms and legs) and short bones (hands, wrists, feet and ankles) of the upper and lower extremities undergo endochondral ossification; a process by which hyaline cartilage is converted to bone. This process begins during early gestation and continues through puberty and into early adulthood until skeletal maturity (18–25 years) when all of the cartilage is replaced by bone. Therefore, in comparison with adults, paediatric bones are more porous and have wider Haversian canals in addition to containing a large amount of collagen and cartilage.¹ Extremity imaging of patients during infancy poses a unique challenge owing to the low intrinsic contrast during skeletal bone development. When considering optimization of extremities in this age range, an understanding of the unossified cartilaginous skeleton is essential.

Extremity imaging at Evelina London Children's Hospital (ELCH), London, UK, is undertaken through various routes of referral and clinical indicators, including trauma and orthopaedic imaging (the identification of fractures or

other bony injuries), genetics (ossification/growth of the bones) and oncology. Perhaps the most significant in the context of this study is the referral of patients for skeletal survey imaging, which incorporates both genetic and non-accidental injury (NAI) pathways. With an increased demand for NAI imaging within the establishment, radiology consultants who report all the imaging undertaken in ELCH, identified some ankle imaging of infant patients (0–1 year old) as undiagnostic, with particular reference to reduced image contrast where it was felt that a loss of clinical features caused subsequent difficulty in making confident clinical decisions. Occasionally repeat imaging was requested, with radiographers adjusting their individual imaging parameters in pursuit of an image providing clarity between the soft tissue and bone regions within the image.

Paediatric patients are more susceptible than adults to the damaging effects of ionizing radiations owing to more rapid cell division and a longer life expectancy.² The lack of

inherent contrast in paediatric extremity imaging is therefore also met by a requirement for optimization of the imaging parameters to ensure the radiation dose to the patient is kept “as low as reasonable achievable” (ALARA).³ Optimization may also minimize the number of requests for repeat imaging, hence reducing the radiation dose and therefore risk to the paediatric patient. In the context of paediatric trauma,⁴ planar X-ray imaging is still considered to be the primary imaging investigation of choice owing to its ready availability and cost effectiveness. Additionally, the Royal College of Radiologists indicate that for focal bone pain in paediatrics, plain film imaging is recommended as the first line of investigation in the evidence-based guidelines “Making the best use of clinical radiology”,⁵ the standards upon which all referrals are subject to in terms of justification.

In conventional screen–film radiography, a fixed detector dose is required to achieve the correct optical density and therefore produce a useable clinical image. European guidelines⁶ published in 1996 have influenced the setting of exposure parameters across the range of different radiographic views. This guidance covers some of the most frequent anatomical projections, including projections of the chest, skull, pelvis, full and segmental spine, abdomen and urinary tract. The general guidance recommends using a higher tube potential (kV) for all radiographic exposures of paediatrics. For older tube-generator systems where the shortest exposure times are not possible, slight lowering of the tube potential and the use of additional filtration is recommended to achieve the required optical density. It states “The soft part of the radiation spectrum which is completely absorbed in the patient is useless for the production of the radiographic image and contributes unnecessarily to the patient dose”. There is evidence suggesting that a harder beam quality in screen–film radiology can result in a lower effective dose (ED) for projections including posteroanterior projections of the chest and anteroposterior (AP) projections of the abdomen.⁷ However, a potential consequence of this dose reduction is a negative effect on the image quality (IQ) as a harder beam results in reduced inherent image contrast as less of the X-ray photons in the spectrum interact via photoelectric absorption.^{7,8}

The International Commission on Radiological Protection (ICRP) have identified the need for optimization and development of consistent protocols in paediatric digital radiology with active participation of staff from a wide range of disciplines.⁹ Direct digital radiography (DDR) is fundamentally different from screen–film radiography in that it has a different energy response and does not require a fixed detector dose, and images can be processed post exposure. Numerous studies have been completed comparing the clinical IQ of extremity radiographs between screen–film and computed radiography (CR)^{10–12} and additionally looking at the possibility of dose reduction in skeletal imaging using amorphous silicon flat panel detectors.^{13,14} However, there is little published evidence to confirm that current protocols are optimized for a wide range of X-ray projections, including extremity imaging.

There have been some optimization studies completed in areas such as cardiac imaging using a flat panel detector¹⁵ and paediatric chest, abdomen and pelvis radiography using CR,¹⁶ but

there is very little literature available on optimization in paediatric extremity imaging. Work by Hess and Neitzel¹⁷ questions the use of filtration and suggests tube potentials as low as 40 kV_p and the removal of any additional filtration can improve the IQ in extremity radiographs of very young patients whilst keeping a fixed ED. This is a phantom study that simulates a paediatric extremity using polymethyl methacrylate representing soft tissue and an aluminium strip representing bone. The study by Brosi et al¹⁶ also questions the benefit of additional copper (Cu) filtration, particularly for radiographic projections that exclude any radiosensitive organs from the primary beam. The study concludes that a reduction in entrance surface dose (ESD) owing to the Cu filtration is not accompanied by a reduction in the ED, which is a true measure of patient risk. An extremity of an infant represents very little attenuation of the beam and the dominant radiosensitive tissue in these projections is the bone marrow according to the ICRP report 103² tissue-weighting factors. For such small structures as the infant extremity, the ratio of the ED to ESD is relatively constant across the tube potential range and actually decreases slightly at the lower tube voltages.¹⁷

Despite the possible benefits of DDR and the scope for optimization in paediatric extremity imaging, it is likely that the current protocols originate from a combination of the European guidance,⁶ manufacturer’s advice and local input from experience with screen–film and possibly CR systems. Moore et al¹⁸ highlight that the anatomically programmed radiography presets on equipment provided by manufacturers may not be appropriate for paediatric exposures. Image optimization in digital radiography requires collaboration between the range of professions associated with the clinical sites and, additionally, the equipment manufacturers. Successful collaboration should result in high-quality digital radiographs being consistently achieved, whilst ensuring automated anatomical programme presets are in keeping with the ALARA principle. The literature review completed as part of this study suggests clinical IQ of extremity radiographs could potentially be improved by lowering the beam quality without resulting in a dose penalty to the patient.

Prior to this study, the local set-up for a lateral ankle exposure of a patient in the 0–1 year (infant) age range at ELCH was 55 kV and 0.1-mm Cu filtration. The aim of this article is to assess the effects of altering tube potential and filtration, with the object of improving contrast and overall IQ, whilst keeping the ED fixed. The intention is to verify the results of Hess and Brosi using an anthropomorphic phantom and audit of clinical images.

METHODS AND MATERIALS

Imaging system and default conditions

All tests were performed at ELCH, which is equipped with a Siemens Axiom Aristos MX (Siemens Medical Solutions, Erlangen, Germany) over-couch X-ray system. The Trixell Pixium 4600 DDR detector (Trixell, Morains, France) that is used by this unit has a caesium iodide phosphor coupled to an array of photo-detectors with a pixel pitch of 0.143 mm.

The system has paediatric anatomical presets for age ranges 0–1, 1–5, 6–10 and 15 years. The default exposure conditions for a lateral ankle radiograph of a patient in the 0–1 age range as set

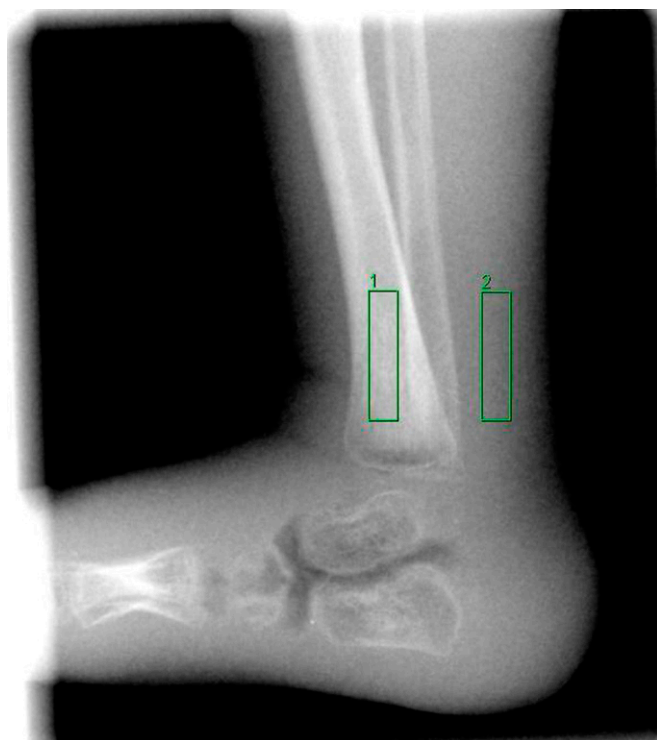
by the manufacturer, with local agreement, were 55, 0.1 mm Cu and 1.4 mAs. These default settings required a fixed focus-to-detector distance of 100 cm, with the beam collimated to the limb. The phantom was positioned and imaged to replicate a true lateral ankle including the distal third of the tibia and fibula with inclusion of the base of the fifth metatarsal as indicated in the radiograph in Figure 1. The detector was situated under the table, and the anti-scatter grid was removed. The dose to the patient from this exposure can be defined in numerous ways; the incident air kerma, the ESD (which is the dose to the skin including backscatter) and the ED. The ED is the most appropriate dose for quantification of stochastic risk, and it can be computed for a known entrance air kerma from Monte Carlo simulation software such as PCXMC v.2.0,¹⁹ this uses the tissue-weighting factors described in ICRP report 103.² Selection of the paediatric “phantom age” was available on the software, and in the case of this study, a 1-year-old phantom age was selected. The phantom used in the software does not have extremities and therefore the X-ray field was positioned to cover the distal end of the lower leg.

Study phantom

PCXMC v.2.0 was used to calculate the ED for a fixed entrance air kerma at each beam quality. The tube output was measured at each beam quality using an Unfors Xi solid state detector (Unfors Instruments, Billdal, Sweden).

The anatomical foot phantom used in the study was manufactured using water equivalent (WT1) material (St Bartholomew’s

Figure 1. Default lateral exposure of infant phantom with an indication of the region of interest (ROI) in the bone (ROI_{bone}) (1) and in soft tissue (ROI_{soft}) (2) used to calculate the contrast-to-noise ratio.



Hospital, London).²⁰ Paediatric skeletal structures, including the tibia and fibula, tarsals and phalanges, were set into this material to create an accurate representation of a true paediatric foot. The size of the phantom is consistent with that of an infant of an age between 0 and 1 year. The phantom was exposed to six different preset tube potentials in the range 40.0–64.5, with and without the presence of a 0.1-mm Cu filter. The standard measurement geometry discussed in the Imaging system and default conditions section was used for all exposures. In order to maintain the fixed ED across a range of beam qualities, the tube current-time product (mAs) had to be modulated for both the variance in computed ED on PCXMC and the variance in the measured tube output.

Phantom image quality assessment

Image quality quantification

Variation of the beam quality can have a direct influence on both the image contrast and image sharpness. In order to define an appropriate parameter to quantify the IQ, both contrast and sharpness need to be considered.

Patient movement has to be considered as a possible cause of image sharpness degradation, particularly in the imaging of paediatric patients. The default tube current on the Siemens Axiom Aristos system for an infant lateral ankle exposure was 220 mA. The exposure time for the range of mAs settings in this study therefore varies between 2.3 and 16.4 ms. These short exposure times should not result in blurring owing to motion, particularly if local immobilization protocol is correctly followed.

In the case of lateral images of the ankle, the radiologists reported low image contrast that was causing difficulty in differentiation between the cortexes of the tibia and surrounding soft tissue. The lack of clarity left the clinicians diffident in making clinical decisions, leading to lateral ankle images being deemed suboptimal and requiring a repeat X-ray for clinical decision-making purposes.

It was decided that the contrast-to-noise ratio (CNR) was the most appropriate measure to assess the effect of changes in beam quality on IQ.⁸ This approach to quantitative IQ assessment has been successfully adopted in other comparable optimization studies.^{15,17,21} The CNR relates to the contrast/signal difference between the structure of interest and the background and can be measured using pixel values in an image that contains a particular contrast detail of interest.

Contrast-to-noise ratio measurements

The images of the phantom at each beam quality were minimally processed by setting processing “gain” values to zero, selecting a linear “look-up-table” and removing the Siemens Diamond View multiresolution spatial filter processing software. However, the “amplification” was set to the default amplification value for the default beam quality (55; 0.1 mm Cu). These settings were necessary to ensure that the signal transfer properties of the system remained consistent. The images were sent to a picture archiving and communication system (PACS) for region of interest (ROI) analysis in order to calculate the CNR at each beam quality. The system use was GE Centricity™ Enterprise Web PACS (GE Healthcare).

The CNR for the purpose of this investigation was defined as shown in Equation (1), where S is the signal in Regions 1 and 2, and σ_1 is the standard deviation (noise) in Region 1.

$$\text{CNR} = \frac{(S_1 - S_2)}{\sigma_1} \quad (1)$$

S_1 and S_2 were defined as a rectangular ROI placed in the central lower region of the tibia and an identical sized ROI in the soft tissue located in a position posterior to the tibia. The positioning of the ROIs is demonstrated in Figure 1. The average number of pixels in the traced ROIs for the 12 images was 1979 ($\sigma = 5$). The reproducibility of the pixel values in the regions was checked for default exposure. The ROI was moved into position five times in each case, and the mean measured signal in ROIs 1 and 2 and noise in ROI 1 were recorded. Using these measurements, the CNR for the default settings was calculated as 7.6 ($\sigma = 0.7$). The measured CNR values (CNR_m) were corrected for the ratio between the calculated mAs (mAs_1) values and set mAs (mAs_2). This was required as the set mAs could only be adjusted to discreet preset values. For a quantum noise-limited system, the CNR is proportional to the square root of the dose. A corrected CNR, CNR_{cor} , was calculated using the relationship described by Equation (2).

$$\text{CNR}_{\text{cor}} = \text{CNR}_m \times \sqrt{\left(\frac{\text{mAs}_1}{\text{mAs}_2}\right)} \quad (2)$$

In order for Equation (2) to be valid, a quantum noise-limited system is required.⁸ The Trixell Pixium 4600 DDR detector is assumed to be quantum noise limited over the range of receptor doses used in this study. A comparative technical report²² states that the detective quantum efficiency (DQE) of this Trixell detector varies by a maximum of 10% over the frequency range 0.5–4.0 cycles mm^{-1} between doses of 1.1 and 11.4 μGy . Quantum noise is therefore suggested to be dominant across this dose range. Borasi et al²³ also confirm this and measure a maximum peak DQE deviation of 15% between doses ranging from 0.91 to 9.31 μGy .

The receptor doses in this investigation were indicated by placing the Unfors Xi detector under the foot phantom so that the tibia and fibula crossed the detector element perpendicularly. The default receptor dose was measured as 7.0 μGy and all receptor doses across the tube potential range used in this investigation were within 20% of this value. The corrections made to the mAs were small, with the maximum correction being 12.9% for the 64.5 and no added Cu exposure (0.50–0.44 mAs). The effect on the CNR correction of any slight deviation from quantum noise-limited behaviour of the detector can be seen to be very small.

Subjective clinical image quality assessment of phantom images

Exposures were made of the anthropomorphic phantom at each beam quality in an identical manner to that discussed for CNR evaluation. However, no changes were made to the automated default clinical pre-processing and display settings, and the images were transferred directly to PACS. This was necessary in order to simulate the exact process that occurs for true clinical images. All of the images were also sent with the Diamond View

algorithm “11—Extremities” (DV11) turned on, and therefore there were 24 images in total. This particular algorithm is occasionally selected by the radiographers, hence its inclusion in this study. The images were randomized in order and were interpreted independently with observers blinded to the variation in beam quality. A subjective assessment of clinical IQ was completed by four trained observers; in this case, three consultant radiologists and one reporting radiographer. Guidelines for assessing basic aspects of quality have been laid out by the European Commission⁶ for a range of projections and paediatric age ranges. However, extremity imaging has not been covered. The ideal set of parameters to describe IQ should measure the effectiveness with which an image can be used for its intended purpose.²⁴ The general scoring framework set out in this study follows the European guidelines although the IQ criteria have been set on the specific diagnostic requirements of paediatric extremity imaging, as defined by the clinicians at ELCH. As discussed previously, the primary issue with the IQ of the radiographs using the default parameters is the difficulty in differentiating between the cortex of the tibia and surrounding soft tissue. Therefore, the visibility of the cortex and the trabecular pattern, which is required to identify any unexpected disruption, is essential.

The image sharpness (X1), image noise (X2) and the perceived visibility of the cortex and trabecular pattern (X3) were all assessed as unacceptable, suboptimum or optimum and given a corresponding IQ score of 1, 2 or 3 for each assessment, respectively. Finally, the overall clinical acceptability (X4) was determined as not acceptable, probably acceptable or fully acceptable, and also given an integer IQ score of 1, 2 or 3. Each of these IQ indices relates to overall exposure and contributes to the radiographic assessment of the image. All indices were equally weighted, assuming that they are of equal significance clinically. The mean score was taken for each criterion across the four observers, and these mean scores summed to give a total score for each. The summing of all four mean criterion scores provides a possible total mean IQ score range of 4–12 with a maximum score of 12 representing all criteria being determined to be imaged optimally by all scorers.

Verification using clinical images of real patients

Once an optimum beam quality was established, the final step was to perform a service audit to verify that the improvement was evident on clinical images. Post-mortem patients were selected who had both ankles imaged as part of a skeletal survey. The mean age of the subjects at the time of imaging was 6.2 months with an age range of 1–15 months. 10 images were acquired on post-mortem patients using the new optimized technique and compared with 10 images previously acquired using the old technique on a different group of patients. No additional imaging was performed on any individual. Five observers were asked to score the images in an identical manner to that described in the Contrast-to-noise ratio measurements section. In this verification, the observers consisted of four consultant radiologists and one reporting radiographer. Once again, the order of the images was randomized, and all images were anonymized. Observers were blinded to the variation in beam quality.

RESULTS

Dosimetry

The ED resulting from an exposure under the default conditions (55; 1.4 mAs) in this study is $0.06 \mu\text{Sv}$, calculated using PCXMC. Radiation dosimetry of the paediatric extremity has also been previously attempted by assessing the energy imparted to a homogeneous slab of water, and the value scaled for the difference in mass between an adult and child.²⁵ The upper limit on the ED for an ankle exposure of a 1-year-old patient was calculated to be $0.31 \mu\text{Sv}$, and this is in agreement with the ED measured from this study when accounting for change in exposure factors to 58 and 6 mAs.

This dose is low in comparison with other radiographic projections as would be expected for an infant extremity exposure; however, the primary purpose of this work was to investigate the possibility of improving IQ, specifically image contrast.

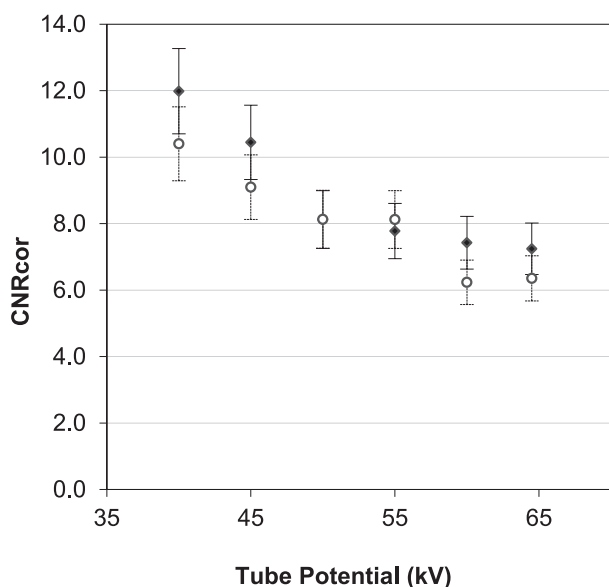
Contrast-to-noise ratio measurements

The CNR_{cor} is shown in Figure 2 across the range of tube potentials and with and without 0.1-mm Cu filtration. The highest CNR_{cor} [11.98 ($\sigma = 0.87$)] was measured on the image taken at the lowest tube potential (40) without the Cu filtration. The CNR_{cor} at this beam quality is 48% higher than the CNR_{cor} measured from the image using the default 55 and 0.1-mm Cu set-up.

Clinical image quality of phantom images

The clinical image qualities of the radiographs of the phantom were assessed using the criterion set out in the Contrast-to-noise ratio measurements section. The mean total IQ scores of all four observers are shown in Figure 3a,b, where Figure 3b

Figure 2. Corrected contrast-to-noise ratio (CNR_{cor}) measurements at a range of beam qualities for the default fixed effective dose of $0.06 \mu\text{Sv}$. The empty circles and solid diamonds indicate 0.1 mm of added copper (Cu) and no added Cu, respectively.



demonstrates the effect of the DV11 pre-processing algorithm. The correlation between the mean scores of each of the four IQ indices was assessed by calculating the Spearman's rank correlation coefficient as displayed in Table 1. The coefficient of variation (CoV) across the mean scores of each IQ index and the total IQ are displayed in Table 2. The variation across the four observers in the mean total IQ score was also assessed using the CoV, and these results are displayed in

Figure 3. Phantom image quality assessment: total image quality (IQ) score for (a) the range of potentials with and without 0.1-mm copper (Cu) and (b) the range of tube potentials with and without 0.1-mm Cu but with the inclusion of DV11. The empty circles and solid diamonds indicate 0.1 mm of added Cu and no added Cu, respectively.

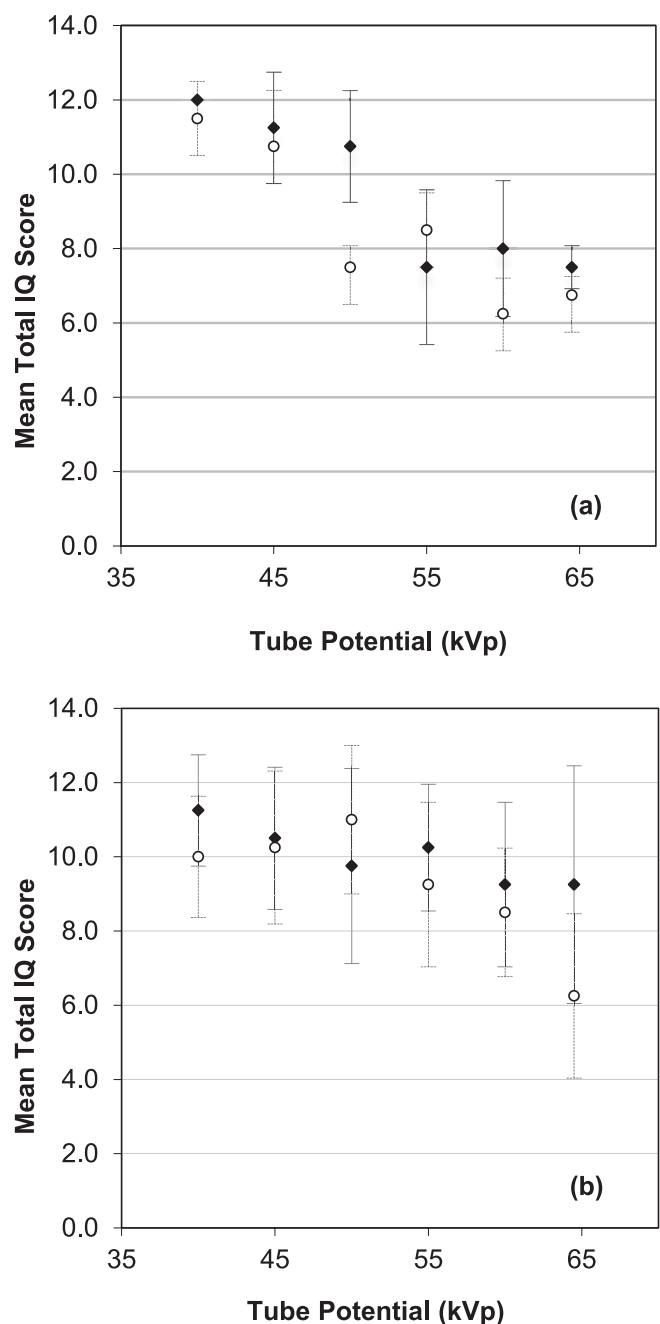


Table 1. Spearman's correlation coefficients between the mean scores of each image quality index of the phantom images

Image group	Image quality indices		R^2	Rank of correlation
All images	X1	X2	0.478	6
	X1	X3	0.842	3
	X1	X4	0.918	1
	X2	X3	0.491	5
	X2	X4	0.561	4
	X3	X4	0.855	2
Without DV11	X1	X2	0.765	6
	X1	X3	0.896	3
	X1	X4	0.959	1
	X2	X3	0.784	5
	X2	X4	0.811	4
	X3	X4	0.947	2
With DV11	X1	X2	0.568	5
	X1	X3	0.777	2
	X1	X4	0.824	1
	X2	X3	0.431	6
	X2	X4	0.705	4
	X3	X4	0.767	3

X1, image sharpness; X2, image noise; X3, perceived visibility of the cortex and trabecular pattern; X4, overall clinical acceptability.

The coefficients are displayed separately for the correlation in indices over all images taken at all beam qualities with and without DV11, images without DV11 and images with DV11.

Table 3. The mean CoV of the mean IQ scores was 17.4% (0–35.5%).

The results clearly indicate that the highest overall IQ score was given to the exposure made using 40 and no additional filtration. Therefore, the subjective IQ assessment is in agreement with the quantitative assessment of the CNR. The inclusion of DV11 does not suggest an improvement in IQ at the lower tube potentials. However, at tube potentials of >55, it could have a positive effect on the clinical IQ.

Verification of optimum beam quality using patient images

The clinical IQ of 10 images obtained using the default beam quality (55, 0.1 mm Cu, 1.4 mAs) and 10 images obtained using the trial beam quality (40, no Cu, 2.5 mAs) was assessed using the methodology discussed in the Contrast-to-noise ratio measurements section. The default tube current was 220 mA resulting in exposure times of 6.4 and 11.4 ms for the default and trial beam qualities, respectively. The mean IQ scores of each criterion (X1–X4) and the total mean IQ scores across the five observers are displayed in Table 4. The mean and standard deviation of the mean total IQ scores for the 10 images acquired using the default beam quality and 10 images acquired using the trial beam quality were 7.9 ($\sigma = 0.8$) and 11.6 ($\sigma = 0.3$), respectively. The variation across the five observers in the mean total IQ score was assessed using the CoV, and these results are also displayed in Table 4.

DISCUSSION

Optimum set-up

The pre-existing local settings for infant extremity (ankle) exposures originate from a combination of the European guidance, input from manufacturers and local optimization strategies. The existing European guidance⁶ for paediatric radiology is based on screen–film detector systems and recommends the use of additional filtration for the majority of projections covered. It also provides a recommended range of tube potentials for each of these planar exposures, none of which fall below 60 kV_p. Although extremity imaging is not specifically mentioned in these guidelines, the results of this study are contradictory to the general advice and suggest that improvements can be made to the IQ through changing the current local protocol. There is an opportunity to exploit the improved CNR and clinical IQ at 40 with no added Cu filtration. Locally, this has been used to achieve a required IQ improvement but equally could have been used to reduce patient dose. The IQ improvements are likely to be seen in a range of extremity radiographic projections of infants and could possibly be extended to different paediatric age ranges. However, further optimization studies will be required for verification.

Lowering the average energy of the spectrum leads to a larger proportion of the photons interacting via photoelectric absorption. This results in an improvement in the inherent contrast in the image⁸ and therefore an increase in the measured CNR. However, lowering the mean energy of the spectrum leads to more absorption in the patient and less photon fluence at the detector. The

Table 2. Coefficient of variation between the mean scores of the four image quality indices and the mean total image quality score of the phantom images

Image quality index	Coefficient of variation		
	All images	Without DV11	With DV11
X1	0.214	0.258	0.158
X2	0.126	0.142	0.100
X3	0.156	0.173	0.139
X4	0.314	0.416	0.196
Total	0.185	0.229	0.138

X1, image sharpness; X2, image noise; X3, perceived visibility of the cortex and trabecular pattern; X4, overall clinical acceptability. Results are displayed separately for all 24 images, 12 images without DV11 and 12 images with DV11.

use of additional Cu filtration can be utilized to harden the beam and reduce patient dose. Huda²⁶ suggests that the main indication for the use of additional Cu filtration in paediatric radiology is to reduce the skin dose during complex interventional procedures. However, deterministic effects such as skin erythema are not a realistic concern in paediatric planar imaging, and the key patient risk is actually the stochastic process of carcinogenesis.

In certain paediatric planar radiographic projections that include superficial radiosensitive tissue, such as the breast tissue, the ED can be reduced when adding Cu filtration and increasing the beam quality. However, Brosi et al¹⁶ report that a reduction in ESD is not accompanied by a reduction in ED when including additional Cu filtration into the beam in DDR of the pelvis and abdomen. The beam hardening reduces the dose to superficial organs but leads to an increased dose to more deep-lying structures. An extremity of an infant patient (0–1 year old) represents very little attenuation of the beam, and the main tissue structure of interest in computing the ED is the bone marrow. For lateral exposures of an infant ankle, the ratio of the ED per unit air kerma at 55 with 0.1 mm Cu (default) to 40 with no added Cu (optimum) is 1.9, *i.e.* the lower energy spectrum results in a lower bone marrow dose and therefore lowers the ED. The mAs can therefore

Table 3. Coefficient of variation (CoV) in the mean total image quality scores of the phantom images across the four observers at each beam quality

kV _p	CoV			
	No Copper		With Copper	
	No DV11	DV11	No DV11	DV11
40.0	0.000	0.133	0.087	0.163
45.0	0.133	0.182	0.140	0.201
50.0	0.140	0.270	0.077	0.182
55.0	0.278	0.167	0.118	0.240
60.0	0.228	0.240	0.153	0.204
64.5	0.077	0.346	0.074	0.355

Results are displayed separately for all beam qualities with and without the inclusion of DV11.

be increased for the lowest beam quality, whilst keeping the ED fixed. The result is an improvement in the contrast and consequently the CNR.

The phantom IQ scores displayed in Figure 3 are in agreement with the quantitative IQ assessment. All three radiologists and the reporting radiographer involved in the IQ assessment each independently scored the image at 40 kV_p, no Cu with a maximum of 12 out of 12, and therefore selected it as the optimum spectrum. The strongest positive correlation across the scores of the 12 images without the inclusion of DV11 was between sharpness and overall acceptability ($R^2 = 0.959$), closely followed by cortex/trabecular pattern with overall acceptability ($R^2 = 0.947$). The improved contrast and therefore visibility of the cortex/trabecular pattern at the lower energy spectrum is also likely to improve the perceived image sharpness, hence the strong positive correlation ($R^2 = 0.896$) between these indices. An improvement in the contrast and sharpness as the beam quality is reduced, therefore directly translates to an increase in likelihood that the overall acceptability is determined as fully acceptable. The mean overall acceptability score over all images had the highest CoV (41.6%) out of all four IQ indices and therefore is likely to have a dominant effect on the overall score. The images that achieved an overall acceptability score of two or three (*i.e.* probably acceptable or fully acceptable) were all at a tube potential ≤ 50 kV_p.

The inclusion of DV11 does not result in an improved mean IQ score at the optimum beam quality setting determined by this study. However, in five out of six images exposed using a tube potential of >55 kV_p, the inclusion of DV11 led to an improved mean IQ score. The specifics of how DV11 changes the images are not freely available, but this study indicates that it is likely that the improvements are only seen at higher tube potentials. It is recognized that the effect of image processing has not been fully investigated in this study. Further work is required to fully evaluate image processing settings and investigate the effect they might have on the conclusions of this study.

The same pattern of correlation between the three indices discussed previously (X1, X3 and X4) was also evident in the DV11 images. However, the correlation was not as strong which is

Table 4. Mean post-mortem image quality scores across five observers for ten images taken using the default beam quality and ten images using the trial beam quality

Image number	Exposure parameters	X1	X2	X3	X4	Total image quality	Coefficient of variation
1	55 kV _p , 0.1 mm Cu, 1.4 mAs	1.4	2.0	1.8	1.0	6.2	0.135
2		1.6	2.0	1.8	1.2	6.6	0.173
3		2.0	2.0	2.2	1.8	8.0	0.234
4		2.0	2.2	2.0	2.2	8.4	0.274
5		2.0	2.2	2.2	2.0	8.4	0.136
6		2.0	2.2	2.4	2.2	8.8	0.095
7		2.0	2.0	2.2	1.6	7.8	0.107
8		2.0	2.0	2.2	1.6	7.8	0.107
9		2.0	2.2	2.0	2.2	8.4	0.065
10		2.0	2.2	2.0	2.2	8.4	0.065
1	40 kV _p , no Cu, 2.5 mAs	2.8	3.0	3.0	2.8	11.6	0.077
2		2.6	3.0	3.0	2.6	11.2	0.098
3		3.0	3.0	3.0	3.0	12.0	0.000
4		3.0	3.0	3.0	3.0	12.0	0.000
5		3.0	2.8	3.0	3.0	11.8	0.038
6		3.0	3.0	3.0	3.0	12.0	0.000
7		2.6	3.0	2.8	2.8	11.2	0.116
8		2.8	3.0	2.8	2.8	11.4	0.118
9		2.8	3.0	3.0	2.8	11.6	0.077
10		2.8	3.0	3.0	2.8	11.6	0.077

Cu, copper; X1, image sharpness; X2, image noise; X3, perceived visibility of the cortex and trabecular pattern; X4, overall clinical acceptability. The coefficient of variation in the mean total image quality score across the five observers is displayed for each image.

indicated by a maximum R^2 value of 0.824 between resolution and overall acceptability. There is no evidence to suggest that DV11 inclusion leads to an improved IQ in extremity imaging of infant patients. The results of this study indicate that for a lowered beam quality (40 and no Cu), removal of DV11 is favourable. The benefits of DV11 and other post-processing tools should be investigated to ensure that they are suitable to the requirements of the specific investigation.

The maximum CoV between the observers total IQ score was 35.5% (Table 3), which occurred in the scoring of the 64.5 kV_p, 0.1 mm Cu and DV11 image. The observers in this case scored the image total IQ as 4, 5, 7 and 9 (mean, 6.25). A CoV of 0% was measured for the 40 kV_p, no Cu image which achieved 12 out of 12 by all observers. The CoV is generally lower for the lower kV_p exposures and also for those without DV11. There is an improved IQ in these exposures owing to a significant improvement in the sharpness of the cortical bone, which provides differentiation between cortex and soft tissue and the presence of a defined trabecular pattern not previously demonstrated. This improvement enables a more confident approach to reporting in the identification or exclusion of pathology and fracture, hence the associated decrease in the score variation.

Verification

The results of the clinical IQ comparison clearly indicate that the IQ at the proposed beam quality is superior to those taken using the default beam quality.

The probability that these results would have been attained if there was no difference in the images is <0.1% as indicated by a two-tailed non-parametric Mann–Whitney U test performed on the two sets of results. None of the 10 mean total IQ scores of the images obtained using the default protocol exceeds the 10 scores of the images obtained using the optimized set-up. These results display clearly that there is a significant improvement in the clinical IQ of the radiographs taken using the lower beam quality and therefore verify the comparable results obtained from the quantitative and qualitative analysis of the phantom images.

The mean CoV in the mean total IQ scores amongst the five observers was measured as 13.9% for the default parameters and 6.0% for the optimized set-up (Table 4). This demonstrates the improved confidence in reporting the images using the new optimized parameters. 3 of the 10 images were scored as a perfect 12 out of 12 by all 5 observers. Reducing the beam quality and improving the inherent contrast not only improves the subjective IQ scores but also reduces the variance in the observer's individual assessments.

In this study, quantitative CNR measurements have been combined with qualitative clinical IQ assessments. It is widely accepted that true optimization is best achieved using task-based measures of IQ.^{27–29} There are a wide variety of examples of studies in the literature utilizing similar qualitative clinical IQ assessment methodologies to that outlined in this article,^{30–32} and it is considered to be likely that the conclusions of this article correlate with the results that would have been seen had a task-based approach been possible.

It is important to recognize that this study does not include a physical measure of resolution. Qualitative scores of sharpness show that the proposed new technique does not have a deleterious effect on perceived sharpness. It should be noted that the new proposed technique could theoretically degrade sharpness as a result of reduced detector modulation transfer function (MTF) or increased patient motion.

The detector resolution is reported to deteriorate slightly when lowering the tube potential.²² In this technical report by Lawinski et al, the modulation transfer function at the Nyquist frequency of a Trixel Pixium detector is reduced from 9.7% to 8.6% when lowering the tube potential from 120 to 70 kV_p. Although measurements were not reported at tube potentials <70 kV_p, theoretically some reduction in MTF between the hardest and softest beams investigated in this study is expected. At lower energies, X-ray photons will tend to interact closer to the surface of the phosphor in the detector. Consequently, the light emitted has further to travel to the photodetector array, resulting in more spread and hence poorer resolution properties. It should be noted that this study was initiated to address concerns raised by radiologists relating to image contrast rather than resolution, therefore it was believed that a small degradation in image sharpness would be tolerable. This is supported by the qualitative assessment of image sharpness of the post-mortem

images, although clearly this does not include any motion artefact effect.

Patient movement needs to be taken into consideration if the results of this study are to be implemented clinically. Movement during exposure can have a negative effect on the sharpness of the final radiograph, as mentioned previously in the Image quality quantification section. The exposure times for the default and optimized beam qualities are reported in the Verification of optimum beam quality using patient images section as 6.4 and 11.4 ms, respectively. European guidance⁶ does not specifically address paediatric extremity imaging; however, it does recommend exposure times <10 ms for AP pelvis, and <20 ms for a lateral skull. In order to eliminate the possible increased motion blur as a result of increased exposure time, one option would be to operate at 45 with no Cu filtration, allowing the exposure time to be reduced to 6.4 ms (1.4 mAs) and maintaining most of the CNR improvement. A second option would be to sacrifice some of the CNR improvement by reducing the mAs. Locally, it is considered that an exposure duration of 11.4 ms is acceptable, and this protocol has been implemented without reports of motion blur.

CONCLUSIONS

The IQ of extremity radiographs of paediatric patients using DDR can be significantly improved by reducing the tube potential to 40 and removing any additional Cu filtration. Results demonstrate that for fixed ED, the softer beam leads to a greatly improved CNR between the tibia and surrounding soft tissue, in lateral projections of a phantom infant foot. These findings have been implemented at ELCH and verified with clinical IQ audit.

FUNDING

This work was supported by Guy's and St Thomas' NHS Foundation Trust, London, UK.

REFERENCES

- Carson S, Woolridge DP, Colletti J, Kilgore K. Paediatric upper extremity injuries. *Pediatr Clin North Am* 2006; **53**: 41–67. doi: [10.1016/j.pcl.2005.10.003](https://doi.org/10.1016/j.pcl.2005.10.003)
- International Commission on Radiological Protection. *The recommendations of the International Commission on Radiological Protection. ICRP report 103*. MD: Elsevier; 2007.
- International Commission on Radiological Protection. Radiological protection and safety in medicine. ICRP report 73. *Ann ICRP* 1996; **26**. doi: [10.1016/s0146-6453\(00\)89195-2](https://doi.org/10.1016/s0146-6453(00)89195-2)
- Sanchez TRS, Jadhav SP, Swischuk LE. MR imaging of pediatric trauma. *Radiol Clin North Am* 2009; **47**: 927–38. doi: [10.1016/j.rcl.2009.08.008](https://doi.org/10.1016/j.rcl.2009.08.008)
- iRefer—focal bone pain in children (P36). Available from: www.rcr.ac.uk
- [\[http://www.irefer.org.uk/index.php/features/paediatrics\]](http://www.irefer.org.uk/index.php/features/paediatrics)
- Council of the European Communities. *European guidelines on quality criteria for diagnostic radiographic images in paediatrics. Report EUR 16261, EN*. 1996; Luxembourg: European Commission.
- Shrimpton PC, Jones DG, Wall BF. The influence of tube filtration and potential on patient dose during X-ray examinations. *Phys Med Biol* 1988; **33**: 1205–12. doi: [10.1088/0031-9155/33/10/009](https://doi.org/10.1088/0031-9155/33/10/009)
- Martin C. The importance of radiation quality for optimisation in radiology. *Biomed Imaging Interv J* 2007; **3**: e38. doi: [10.2349/biij.3.2.e38](https://doi.org/10.2349/biij.3.2.e38)
- International Commission on Radiological Protection. Radiological protection in paediatric diagnostic and interventional radiology. ICRP Publication 121. *Ann ICRP* 2013; **42**: 1–63.
- Wilson AJ, Mann FA, Murphy WA Jr, Monsees BS, Linn MR. Photostimulable phosphor digital radiography of the extremities: diagnostic accuracy compared with conventional radiography. *AJR Am J Roentgenol* 1991; **157**: 533–8. doi: [10.2214/ajr.157.3.1872241](https://doi.org/10.2214/ajr.157.3.1872241)
- Swee RG, Gray JE, Beabout JW, McLeod RA, Cooper KL, Bond JR, et al. Screen-film versus computed radiography imaging of the hand: a direct comparison. *AJR Am J Roentgenol* 1997; **168**: 539–42. doi: [10.2214/ajr.168.2.9016243](https://doi.org/10.2214/ajr.168.2.9016243)
- Kleinman PL, Zurakowski D, Strauss KJ, Cleveland RH, Perez-Rosello JM, Nichols DP, et al. Detection of simulated inflicted metaphyseal fractures in a fetal pig model: image optimization and dose reduction with computed radiography. *Radiology*

- 2008; **247**: 381–90. doi: [10.1148/radiol.2472070811](https://doi.org/10.1148/radiol.2472070811)
13. Strotzer M, Gmeinwieser J, Spahn M, Völk M, Fründ R, Seitz J, et al. Amorphous silicon, flat-panel, x-ray detector *versus* screen-film radiography: effect of dose reduction on the detectability of cortical bone defects and fractures. *Invest Radiol* 1998; **33**: 33–8. doi: [10.1097/00004424-199801000-00005](https://doi.org/10.1097/00004424-199801000-00005)
 14. Völk M, Paetzel C, Angele P, Seitz JS, Füchtmeier B, Hente R, et al. Routine skeleton radiography using a flat-panel detector: image quality and clinical acceptance at 50% dose reduction. *Invest Radiol* 2003; **38**: 230–5.
 15. Gislason AJ, Davies AG, Cowen AR. Dose optimization in pediatric cardiac x-ray imaging. *Med Phys* 2010; **37**: 5258–69. doi: [10.1118/1.3488911](https://doi.org/10.1118/1.3488911)
 16. Brosi P, Stuessi A, Verdun FR, Vock P, Wolf R. Copper filtration in pediatric digital X-ray imaging: its impact on image quality and dose. *Radiol Phys Technol* 2011; **4**: 148–55. doi: [10.1007/s12194-011-0115-4](https://doi.org/10.1007/s12194-011-0115-4)
 17. Hess R, Neitzel U. Optimizing image quality and dose for digital radiography of distal pediatric extremities using the contrast-to-noise ratio. *Rofa* 2012; **184**: 643–9. doi: [10.1055/s-0032-1312727](https://doi.org/10.1055/s-0032-1312727)
 18. Moore QT, Don S, Goske MJ, Strauss KJ, Cohen M, Herrmann T, et al. Image gently: using exposure indicators to improve pediatric digital radiography. *Radiol Technol* 2012; **84**: 93–9.
 19. Tapiovaara M, Siiskonen T. A PC-based Monte Carlo program for calculating patient doses in medical X-ray examinations. Report STUK-A139. Helsinki, Finland: Finnish Centre for Radiation and Nuclear Safety; 1997.
 20. White DR. The formulation of tissue substitute materials using basic interaction data. *Phys Med Biol* 1977; **22**: 889–99. doi: [10.1088/0031-9155/22/5/008](https://doi.org/10.1088/0031-9155/22/5/008)
 21. Moore CS, Beavis AW, Saunderson JR. Investigation of optimum X-ray beam tube voltage and filtration for chest radiography with a computed radiography system. *Br J Radiol* 2008; **81**: 771–7. doi: [10.1259/bjr/21963665](https://doi.org/10.1259/bjr/21963665)
 22. Lawinski C, Mackenzie A, Cole H, Blake P, Honey ID. *Digital detectors for general radiography: a comparative technical report. Evaluation report 05078*. Centre for Evidence-Based Purchasing. 2005.
 23. Borasi G, Nitrosi A, Ferrari P, Tassoni D. On site evaluation of three flat panel detectors for digital radiography. *Med Phys* 2003; **30**: 1719–31. doi: [10.1118/1.1569273](https://doi.org/10.1118/1.1569273)
 24. Martin C. Optimisation in general radiography. *Biomed Imaging Interv J* 2007; **3**: e18. doi: [10.2349/bijj.3.2.e18](https://doi.org/10.2349/bijj.3.2.e18)
 25. Huda W, Gkanatsios NA. Radiation dosimetry for extremity radiographs. *Health Phys* 1998; **75**: 492–9. doi: [10.1097/00004032-199811000-00005](https://doi.org/10.1097/00004032-199811000-00005)
 26. Huda W. Assessment of the problem: pediatric doses in screen-film and digital radiography. *Pediatr Radiol* 2004; **34**(Suppl. 3): S173–82; discussion S234–41. doi: [10.1007/s00247-004-1267-8](https://doi.org/10.1007/s00247-004-1267-8)
 27. Barrett HH, Myers KJ, Hoeschen C, Kupinski MA, Little MP. Task-based measures of image quality and their relation to radiation dose and patient risk. *Phys Med Biol* 2015; **60**: R1–75. doi: [10.1088/0031-9155/60/2/R1](https://doi.org/10.1088/0031-9155/60/2/R1)
 28. Barrett HH. Objective assessment of image quality: effects of quantum noise and object variability. *J Opt Soc Am A* 1990; **7**: 1266–78. doi: [10.1364/josaa.7.001266](https://doi.org/10.1364/josaa.7.001266)
 29. International Commission on Radiation Units and Measurements (ICRU). *Medical imaging—the assessment of image quality. ICRU report no. 54*. Bethesda, MD: ICRU; 1996.
 30. Dougeni ED, Delis HB, Karatza AA, Kalogeropoulou CP, Skiadopoulos SG, Mantagos SP, et al. Dose and image quality optimization in neonatal radiography. *Br J Radiol* 2007; **80**: 807–15. doi: [10.1259/bjr/77948690](https://doi.org/10.1259/bjr/77948690)
 31. Sandborg M, Tingberg A, Ullman G, Dance DR, Alm Carlsson G. Comparison of clinical and physical measures of image quality in chest and pelvis computed radiography at different tube voltages. *Med Phys* 2006; **33**: 4169–75. doi: [10.1118/1.2362871](https://doi.org/10.1118/1.2362871)
 32. Almén A, Tingberg A, Mattsson S, Besjakov J, Kheddache S, Lanhede B, et al. The influence of different technique factors on image quality of lumbar spine radiographs as evaluated by established CEC image criteria. *Br J Radiol* 2000; **73**: 1192–9.